PHYSICAL REVIEW B VOLUME 25, NUMBER 3 1 FEBRUARY 1982

New method for the determination of the sign and magnitude of electric quadrupole splittings. I. Theoretical considerations

E. Hagn
Physik-Department, Technische Universität, München, D-8046 Garching, Federal Republic of Germany
(Received 29 June 1981)

For systems with a small electric quadrupole interaction $\nu_Q = e^2qQ/h$ besides a large magnetic hyperfine splitting $\nu_M = |g\mu_N B_{\rm hf}/h|$ the centers of the NMR-ON (oriented nuclei) resonances are displaced by $\Delta\nu = c\nu_Q$. It is shown that c is different for $\theta = 0°$ and 90°, θ being the angle of observation with respect to the quantization axis. This implies that the magnitude and sign of ν_Q can be determined from the differential resonance displacement $\overline{\Delta\nu} = \overline{\nu(0)} - \overline{\nu(90)}$. Model calculations are performed and the applicability of the method is discussed.

I. INTRODUCTION

The main part of the hyperfine interaction (HI) of nuclei in a ferromagnetic host lattice is the magnetic dipole interaction $\nu_M = g\mu_N B_{\rm hf}/h$. The hyperfine field $B_{\rm hf}$ is known for most elements as dilute impurities in Fe, Co, Ni, and Gd.[1] For nuclei with $j \geq 1$ a (small) quadrupole interaction (QI) $\nu_Q = e^2qQ/h$ may be superimposed to the magnetic interaction. The electric field gradient (EFG) eq arises either from the unquenched orbital momenta of the $3d,4d,5d$ electrons in cubic Fe,Co,Ni or (in addition) from the noncubic crystal structure in hcp Co and Gd. The HI of radioactive nuclei in Fe,Co,Ni has been investigated widely with the NMR-ON technique (nuclear magnetic resonance on oriented nuclei detected via the anisotropy of radiation).[2]

A tabulation of NMR-ON experiments has been given recently.[3] Only for a few exceptional cases the quadrupole splitting could be resolved well.[4] In most cases the linewidth which is mainly caused by inhomogeneous broadening is so large that the quadrupole structure (either $2j$ subresonances or, at least, an asymmetry) cannot be detected. In this paper it will be shown that the magnitude *and* sign of ν_Q can be determined from the 0°−90° differential resonance displacement (DRD) of the NMR-ON resonances, measured at $\theta = 0°$ and 90° with respect to the direction of magnetization, even if the linewidth is much larger than the quadrupole splitting. This is due to the fact that the effective resonance centers depend on the tensor rank k of the quantity under observation. For the γ anisotropy $k = 2$ and $k = 4$ terms are present which are weighted differently for $\theta = 0°$ and 90°. In this way the QI causes a resonance displacement which is different for $\theta = 0°$ and $\theta = 90°$. As the center of a resonance structure can be determined much more easily than a slightly asymmetric structure (no complicated analysis of the measured spectra is necessary), the method seems to be quite promising for the measurement of both EFG's and ground-state spectroscopic quadrupole moments of radioactive nuclei.

The basic principles and a rigorous calculation are presented in Secs. II and III, respectively. For ^{60}Co*Co* (hcp), model calculations have been performed; the results are given in Sec. IV. This system has been chosen as precise experimental data are available.[5] The general applicability of this method will be discussed in Sec. V.

II. THE 0°−90° DIFFERENTIAL RESONANCE DISPLACEMENT: BASIC PRINCIPLES

The angular distribution of γ rays emitted in the decay of oriented nuclei is most conveniently written as[6]

$$W(\theta) = 1 + \sum_{k=2}^{k_{\max}} A_k B_k (\mu B/k_B T) P_k(\cos\theta) Q_k \ . \qquad (1)$$

Here the parameters A_k contain all information about the nuclear decay cascade; they are products of the usual angular correlation coefficients U_k

and F_k, which, e.g., are tabulated in Ref. 7. The B_k describe the degree of orientation. The connection with the sublevel population probabilities a_m is given by

$$B_k=(2j+1)^{1/2}\sum_m(-1)^{j-m}\langle jmj-m\mid k0\rangle a_m\ . \tag{2}$$

The $P_k(\cos\theta)$ in Eq. (1) are Legendre polynomials, θ being the angle between the direction of observation and the quantization axis, and Q_k are solid-angle correction coefficients. Only even k values are allowed in Eq. (1), $k_{\max}$ being fixed by angular momentum selection rules. In most cases $k_{\max}=4$. The γ anisotropy is defined as

$$A(\theta)=W(\theta)-1\ . \tag{3}$$

In NMR-ON experiments the γ anisotropy is used as detector for NMR. For the case of a combined magnetic dipole and electric quadrupole interaction,[8] both being collinear, the resonance frequency for transitions between state $\mid m\rangle$ and $\mid m+1\rangle$ is given by

$$\begin{aligned}
&\nu_{m\to m+1}=\nu_0+\Delta\nu_Q(m+1/2)\ ,\\
&\nu_0=\nu_M+\mid g\mu_N/h\mid(1+K)\mid B_0\mid\mathrm{sgn}(B_{\mathrm{hf}})\ ,\\
&\nu_M=\mid g\mu_N B_{\mathrm{hf}}/h\mid\ ,\\
&\nu_Q=e^2qQ/h\ ,\\
&\Delta\nu_Q=3\nu_Q/[2j(2j-1)]\ .
\end{aligned} \tag{4}$$

Here ν_0 is the "pure" magnetic resonance, as expected in the absence of a quadrupole splitting, ν_M and ν_Q are the usually quoted magnetic dipole and electric quadrupole splittings, respectively. B_0 and B_{hf} are the external magnetic field and the hyperfine field, respectively. K is the Knight-shift parameter, g is the nuclear g factor, eq is the EFG, Q is the spectroscopic quadrupole moment, and $\Delta\nu_Q$ is the quadrupole subresonance separation. It is obvious that a set of $2j$ subresonances is expected, which are separated by $\Delta\nu_Q$.

The response of the nuclear spin system (and thus the corresponding change of the γ anisotropy) depends, however, on the strength of the spin-lattice relaxation, too. This is illustrated in Fig. 1 for $j=1$. Starting from a Boltzmann distribution (left), the population difference of the lower two sublevels is removed if an rf field with frequency ν_1 is applied. (Here it has been assumed that the reduced matrix element, which describes the strength of the rf transition probability, is much larger than the corresponding matrix element of the spin-lattice relaxation process; see Sec. III.) This so-called slow-relaxation limit (SRL) is shown in the middle part of Fig. 1. If the rf field is maintained for a long time in comparison to the spin-lattice relaxation time, a new Boltzmann distribution is obtained, with the constraint that the population probability of the lower two sublevels is equal. This is the so-called fast-relaxation limit

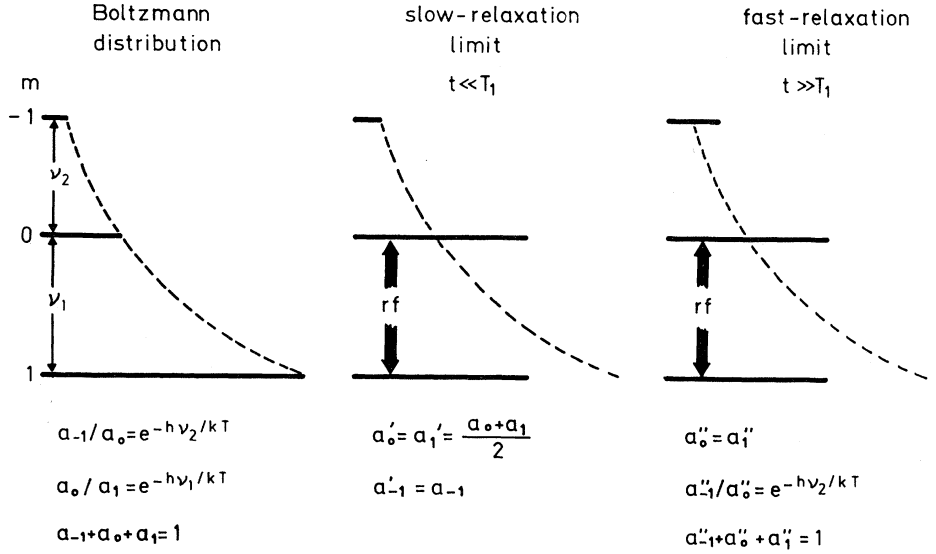

FIG. 1. Response of the nuclear spin system on the application of a (strong) rf field with frequency ν_1. Starting from a Boltzmann distribution (left) the population difference of the lower two sublevels is removed if the rf is switched on (middle: slow-relaxation limit). If the rf is maintained for a long time in comparison to the spin-lattice relaxation time a new Boltzmann distribution is obtained (right: fast-relaxation limit).

(FRL), which is illustrated at the right-hand side of Fig. 1.

For both limits the resonance effect, i.e., the corresponding change of $A(\theta)$, is now calculated with the new sublevel populations utilizing Eqs. (2) and (1). For the resonant change of the γ anisotropy the $k=4$ term in Eq. (1) plays an essential role, as the change of B_4 can be much larger than that of B_2. This can be seen from the B_k coefficients for complete population of state $|m\rangle$ which are given by

$$\bar{B}_k^{(m)}=(2j+1)^{1/2}(-1)^{j-m}\langle jmj-m\,|\,k0\rangle\ . \quad (5)$$

In Table I, $\bar{B}_2^{(m)}$ and $\bar{B}_4^{(m)}$ are listed for $j=5$. It is evident that the changes of B_2 and B_4, ΔB_2 and ΔB_4, respectively, are different. This has the consequence that $\Delta A(0)/\Delta A(90)$ is different for all quadrupole subresonances. (Here only $A_2\neq 0$ and $A_4\neq 0$ has to be assumed.) This has the further consequence that the structure of the observable resonance spectrum must be different for $\theta=0°$ and 90°.

If the inhomogeneous linewidth is so large that neither the quadrupole splitting can be resolved nor an asymmetry of the resonance spectrum can be observed, there still remains a 0°−90° displacement of the observable effective resonance centers from which the quadrupole splitting can be deduced, as will be shown in the following.

Let us denote the resonance which corresponds to the energetically lowest sublevel transition as ν_1 resonance, the next as ν_2 resonance, etc., ν_i, $i=1,\ldots,2j$ and the corresponding changes of the γ anisotropy ΔW_i, $i=1,\ldots,2j$. The effective resonance center is then given by

$$\overline{\nu(\theta)}=\frac{\sum\nu_i\Delta W_i(\theta)}{\sum\Delta W_i(\theta)}\ , \quad (6)$$

TABLE I. Nuclear orientation parameters $\bar{B}_2^{(m)}$ and $\bar{B}_4^{(m)}$ for complete population of state $|jm\rangle$ with $j=5$.

m	$\bar{B}_2^{(m)}$	$\bar{B}_4^{(m)}$
0	−1.1323	+1.1767
±1	−1.0190	+0.7845
±2	−0.6794	−0.1961
±3	−0.1132	−1.1767
±4	+0.6794	−1.1767
±5	+1.6984	+1.1767

with

$$\overline{\nu(\theta)}=\nu_0+c(\theta)\Delta\nu_Q\ . \quad (7)$$

The displacement constant $c(\theta)$ is given by

$$c(\theta)=\frac{\sum(m_i+\frac{1}{2})\Delta W_i(\theta)}{\sum\Delta W_i(\theta)}\ . \quad (8)$$

Denoting

$$\Delta c=c(0)-c(90)\ , \quad (9)$$

the differential resonance displacement $\overline{\Delta\nu}$ of the effective resonance centers at $\theta=0°$ and 90°, $\overline{\nu(0)}-\overline{\nu(90)}$, is given by

$$\overline{\Delta\nu}=\overline{\nu(0)}-\overline{\nu(90)}=\Delta c\Delta\nu_Q\ . \quad (10)$$

A calculation of Δc in both limits described before, SRL and FRL, shows that Δc^{SRL} and Δc^{FRL} differ strongly (see also Sec. IV). This means that a rigorous calculation of Δc is necessary.

III. THE 0°−90° DIFFERENTIAL RESONANCE DISPLACEMENTS RIGOROUS CALCULATION

The starting point is the master equation

$$\dot{a}_m=\sum_m(a_nW_{nm}-a_mW_{mn})\ . \quad (11)$$

Here $a_m(t)$ is the time-dependent sublevel population probability of state $|m\rangle$ and W_{mn} is the total transition probability from state $|m\rangle$ to state $|n\rangle$ which is given by

$$W_{mn}=W_{mn}^{(\mathrm{SL})}+W_{mn}^{(\mathrm{rf})}\ , \quad (12)$$

where $W_{mn}^{(\mathrm{SL})}$ is the contribution from the spin-lattice relaxation, and $W_{mn}^{(\mathrm{rf})}$ describes the transition probability due to the applied rf field. The spin-lattice relaxation contribution is given by[9]

$$W_{m,m+1}^{(\mathrm{SL})}=B^{\mathrm{SL}}h\nu_M\times[j(j+1)-m(m+1)]/(e^{\beta}-1)\ ,$$
$$W_{m+1,m}^{(\mathrm{SL})}=B^{\mathrm{SL}}h\nu_M\times[j(j+1)-m(m+1)]/(1-e^{-\beta})\ . \quad (13)$$

Here B^{SL} is a constant which describes the strength of the relaxation process and $\beta=h\nu_M/k_BT$. [Strictly, $B^{\mathrm{SL}}h\nu_M$ and β should be replaced by $B^{\mathrm{SL}}h\nu_{m,m+1}/h\nu_M$ and $h\nu_{m,m+1}/k_BT$, respectively. As $|(\nu_{m,m+1}-\nu_M)/\nu_M|\ll 1$ is fulfilled

for all cases where the QI cannot be resolved, the "standard" formulas of Eq. (13) can be used.] It can be shown[9] that the connection between the high-temperature Korringa constant $\mathcal{K}$ and the relaxation parameter B^{SL} is given by

$$B^{\mathrm{SL}}=\frac{1}{2k_B\mathcal{K}} . \tag{14}$$

The rf transition probability is given by

$$W_{m,m+1}=(B^{\mathrm{rf}}/\Delta f_t)[j(j+1)-m(m+1)]g_m(\nu_c) ,$$
$$W_{m+1,m}=W_{m,m+1} . \tag{15}$$

Here B^{rf} is a reduced matrix element which is proportional to the rf power at the nuclear sites. It depends on several parameters such as the field strength of the applied rf field and the enhancement factor for the rf field. B^{rf} can be determined experimentally from the time dependence of the γ anisotropy if a resonant rf field is switched on (see Sec. IV). Δf_t in Eq. (15) is the total modulation width of the frequency modulation. The parameter $g_m(\nu_c)$ in Eq. (15) takes into account which transitions can be affected by the rf field of center frequency ν_c. It depends on ν_c and on the modulation width Δf_t. If, e.g., $\nu_c=\nu_{n,n+1}$ and $\Delta f_t<|\Delta\nu_Q|$, then $g_m(\nu_c)=\delta_{m,n}$.

In the absence of a resonant rf field, $B^{\mathrm{rf}}=0$, the steady-state solution of Eq. (11) is the undisturbed Boltzmann distribution:

$$\overline{a_m}=e^{-h\nu_m/k_BT}\Big/\sum_{m'}e^{-h\nu_{m'}/k_BT} . \tag{16}$$

If at time $t=0$ a resonant rf field is switched on, the time dependence of $a_m(t)$ is given by

$$a_m(t)=\sum_{n,1}C_{mnl}e^{-\lambda_1 t}\overline{a_n} . \tag{17}$$

The constants C_{mnl} and λ_1 are calculated by diagonalizing the matrix of Eq. (11), they depend on the temperature T, the relaxation parameter B^{SL}, the rf parameter $B^{\mathrm{rf}}/\Delta f_t$, and on the modulation parameter $g_m(\nu_c)$. The time dependence of the γ anisotropy is then given by

$$W(\theta,t)=\sum_{1}\omega_1(\theta)e^{-\lambda_1 t} . \tag{18}$$

The constants $\omega_1(\theta)$ are calculated with the help of Eqs. (1) and (2).

Suppose now that $g_m(\nu_c)$ is chosen in such a way that only the sublevel transition i (with frequency ν_i) can be affected by the rf. The time dependence of the corresponding sublevel populations is then given by

$$a_m^{(i)}(t)=\sum_{n,1}C_{mnl}^{(i)}e^{-\lambda_1^{(i)}t}\overline{a_n} . \tag{19}$$

Denoting the corresponding time-dependent change of the γ anisotropy

$$\Delta W^{(i)}(\theta,t)=W^{(i)}(\theta,t)-\overline{W(\theta)} \tag{20}$$

[here $\overline{W(\theta)}=W^{(i)}(\theta,t=0)$, the initial value being independent of i] we can now calculate the time dependence of the displacement constant

$$c(\theta,t)=\frac{\sum_i(m_i+\frac{1}{2})\Delta W^{(i)}(\theta,t)}{\sum_i\Delta W^{(i)}(\theta,t)} \tag{21}$$

and hence

$$\Delta c(t)=c(0,t)-c(90,t) . \tag{22}$$

For a given measurement time Δt the average displacement is calculated by integration:

$$\overline{c(\theta)}=\frac{\int_0^{\Delta t}\sum_i(m_i+\frac{1}{2})\Delta W^{(i)}(\theta,t)dt}{\int_0^{\Delta t}\sum_i\Delta W^{(i)}(\theta,t)dt} . \tag{23}$$

The average differential displacement constant $\overline{\Delta c}$ is again given by

$$\overline{\Delta c}=\overline{c(0)}-\overline{c(90)} . \tag{24}$$

By setting $a_m^{(i)}(t=0)=\overline{a_m}$ in Eq. (19) [and hence $W^{(i)}(\theta,t=0)=\overline{W(\theta)}$ in Eq. (20)], it has been assumed tacitly that between two measurements (at different frequencies) a waiting period is included (with the rf power being switched off) during which the spin system can return to the thermal equilibrium. Experiments performed in this way would be ineffective, as too much measurement time would be lost. In the so-called sweep-mode technique[10] the rf frequency is varied continuously over the resonance region with a sweep rate ρ (unit: frequency per time). Let us first consider the special case $\Delta f_t=|\Delta\nu_Q|$. Here the resonance ν_{i+1} is entered immediately after resonance ν_i has been passed. This means that the effective integration time Δt in Eq. (23) has to be replaced by $\Delta t_s=|\Delta\nu_Q|/|\rho|$. (This is the time interval during which one subresonance can be affected by the rf.) In addition, the initial values for the sublevel populations $\overline{a_n}$ in Eq. (19) have to be replaced by $a_n^{(i-1)}(t=\Delta t_s)$. It is obvious that the result for $\overline{\Delta c}$ now depends on the sweep direction; i.e., on the se-

quence $i-1,i,i+1,\ldots$, in which the different subresonances are entered. (This sequence is reverse for sweep-up and sweep-down.) If ρ is chosen in such a way that Δt_s is small in comparison to the spin-lattice relaxation time, a large difference for $\overline{c(\theta)}$ and $\overline{\Delta c}$ (and the respective resonance amplitudes) is to be expected for both sweep directions. This dependence of $\overline{c(\theta)}$ on the sweep rate ρ implies a further possibility for the determination of $\Delta\nu_Q$. It can then be applied if $\overline{\Delta c}=0$ is expected, which is the case for, e.g., $E1$ or $M1$ γ transitions ($A_4=0$).

For $\Delta f_t < |\Delta\nu_Q|$ and $\Delta f_t > |\Delta\nu_Q|$ the calculations are slightly more difficult. For $\Delta f_t < |\Delta\nu_Q|$ "waiting periods" have to be taken into account; i.e., time intervals during which *no* subresonance can be affected by the rf. For $\Delta f_t > |\Delta\nu_Q|$ it has to be taken into account that n subresonances may be affected simultaneously by the rf. (The number n is not necessarily constant.) No decisive differences are expected for $\Delta f_t < |\Delta\nu_Q|$ and $\Delta f_t > |\Delta\nu_Q|$. Finally, we want to note that the sweep-mode average $\overline{\Delta c}$ is expected to be nearer to Δc^{FRL} as the "effective" integration time is longer.

IV. MODEL CALCULATIONS FOR ^{60}Co*Co* (hcp)

The decay of ^{60}Co ($j^\pi=5^+$; $T_{1/2}=5.3y$) takes place with 99.9% via the cascade

$$5^+ \xrightarrow{\beta^-} 4^+ \xrightarrow[E2,1.17\ \mathrm{MeV}]{\gamma} 2^+ \xrightarrow[E2,1.33\ \mathrm{MeV}]{\gamma} 0^+ .$$

Both γ transitions at 1173 and 1332 keV have identical A_k coefficients as the γ cascade is stretched ($A_2=-0.420\,56$; $A_4=-0.242\,81$). For all further calculations the magnetic hyperfine splitting of ^{60}Co in hcp Co has been taken

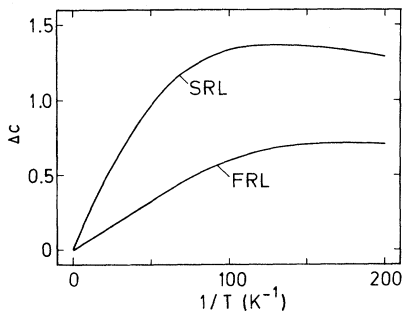

FIG. 2. Differential displacement constant Δc versus $1/T$ for the slow and fast relaxation limits.

$\nu_M=126.8$ MHz,[5] and $Q_k=1$ has been assumed for the solid-angle correction coefficients. Figure 2 shows the DRD constant Δc versus $1/T$, calculated for both limits outlined in Sec. II, slow relaxation (SRL) and fast relaxation(FRL). It is obvious that the full time dependence has to be taken into account to calculate values of Δc which can reliably be used for the interpretation of experimental $0°-90°$ resonance displacements.

In addition to $\nu_{M'}$, for the "exact" calculations B^{SL} and B^{rf} have to be known. (The knowledge of ν_Q is not necessary as $2j\,|\Delta\nu_Q| << \nu_M$ is expected[5]; see also Sec. II). The spin-lattice relaxation parameter B^{SL} has been obtained in the following way. Enokiya[11] measured the high-temperature Korringa constant $\mathcal{K}$ of ^{59}Co in hcp Co to be $\mathcal{K}=0.17(1)$ sec K. The magnetic hyperfine splitting of ^{59}Co*Co* (hcp) in the direction of the c axis—the hyperfine splitting is anisotropic—is known to be $\nu_M=219.9$ MHz.[12] For a pair of isotopes in the same electronic environment, the Korringa constants vary as[13]

$$\mathcal{K}_1/\mathcal{K}_2=(\nu_2/\nu_1)^2 , \tag{25}$$

where $\nu_{1/2}$ are the respective hyperfine splittings. The spins $j_{1,2}$, which may be different, do not enter Eq. (25). In this way $\mathcal{K}(^{60}\mathrm{Co}Co)=0.51(3)$ sec K and hence

$$B^{\mathrm{SL}}=4.7(3)\times10^{-5}\ \mathrm{MHz}^{-1}\,\mathrm{sec}^{-1}$$

is obtained. The rf-frequency coupling parameter B^{rf} cannot be calculated but can be determined experimentally from the time dependence of the γ anisotropy if a resonant rf field is switched on and off.

Figure 3 shows the results of model calculations performed for different values of $B^{\mathrm{rf}}/\Delta f_t$. Here it has been assumed that all quadrupole subresonances can be affected by the rf; i.e., that the γ anisotropy can be destroyed completely if $B^{\mathrm{rf}}/\Delta f_t$ is large enough. Such time-dependent γ anisotropy spectra as simulated in Fig. 3 can easily be measured. The analysis of such spectra is, however, often being performed assuming single-exponential functions with time constants T_R and T_1' for the resonant change and the return of the γ anisotropy to the thermal equilibrium, respectively.

In order to get a feeling for the functional dependence between T_R, T_1', and $B^{\mathrm{rf}}/\Delta f_t$ we have fitted the simulated γ anisotropies as shown in Fig. 3 with such single-exponential functions. The result is listed in Table II. It is obvious that $B^{\mathrm{rf}}/\Delta f_t$ can be determined from the rise-time constant T_R

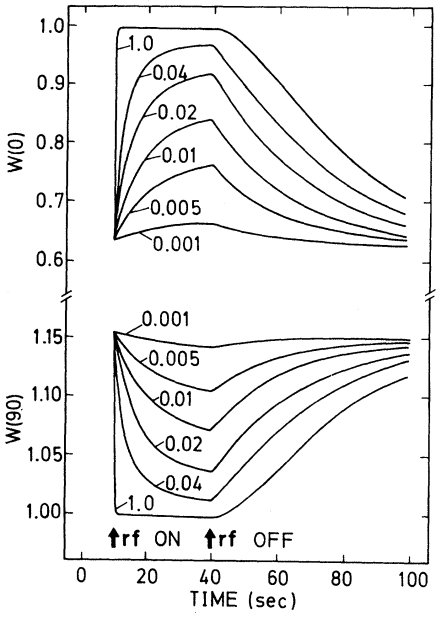

FIG. 3. Model calculations for the time dependence of the γ anisotropy $W(0)$ (top) and $W(90)$ (bottom) if a resonant rf field is switched on and off at $t=10$ sec and $t=40$ sec, respectively. The respective strength of the rf power, $B^{rf}/\Delta f_t$, is given beside each curve (unit: sec^{-1}). The rise of the γ anisotropy for $10<t<40$ sec can be well described by a single-exponential function. The return of the γ anisotropy to the thermal equilibrium for $t>40$ sec is well described with a single-exponential function for $B^{rf}/\Delta f_t \lesssim 0.04$ sec^{-1}. It is evident that $B^{rf}/\Delta f_t$ can be determined experimentally from the rise-time constant and from the resonance amplitude.

and from the resonance amplitude $\Delta W(\theta)$. (In practice only the rise time yields reasonable $B^{rf}/\Delta f_t$ values, as the absolute resonance amplitudes may be influenced by metallurgic properties, thickness of the samples via the skin depth, etc.) From measured rise-time constants on ^{60}Co*Co* (hcp) with $\Delta f_t=1$ MHz of $T_R\sim 4-10$ sec, $B^{rf}/\Delta f_t=0.01-0.04$ sec^{-1} is estimated as a realistic value.

Figure 4 shows the time dependence of the differential resonance displacement constant $\Delta c(t)$ calculated for $B^{rf}/\Delta f_t=0.01$, 0.1, and 1 sec^{-1} and $1/T=100$ K^{-1}. Here it has been assumed that $\Delta f_t=|\Delta\nu_Q|$, i.e., that exactly one subresonance can be affected by the rf. (The rf is switched on at $t=0$.) It is a remarkable fact that the functional dependence of $\Delta c(t)$ on $B^{rf}/\Delta f_t$ is extremely weak. (Because of the finite skin depth the effective rf power may vary considerably within the sample. In this way the observable resonance amplitude may be reduced; the differential resonance displacement is, however, only weakly affected.) For the case of high rf power, $B^{rf}/\Delta f_t=1$ sec^{-1}, $\Delta c(t=0)$ and $\Delta c(t=\infty)$ coincide well with the two limits, Δc^{SRL} and Δc^{FRL} (see Fig. 2).

Figures 5 and 6 illustrate the behavior of $\overline{c(0)}$ and $\overline{\Delta c}$ versus $1/T$ calculated for $B^{rf}/\Delta f_t=0.1$ sec^{-1} and measurement times $\Delta t=4$ and 40 sec, respectively. The curves labeled *b*, *c*, and *d* represent the results of calculations for sweep-mode technique, sweep-up, sweep-down, and sweep-up-down, respectively. (Because of the different resonance amplitudes for both sweep direc-

TABLE II. Rise-time constant T_R, anisotropy relaxation time T_1', and resonance effect r as function of the rf-power parameter $B^{rf}/\Delta f_t$. (Result of single-exponential fits to the model calculations shown in Fig. 3.) For $B^{rf}/\Delta f_t>0.04$, the return of the γ anisotropy to the thermal equilibrium is no longer describable with a single-exponential function.

$B^{rf}/\Delta f_t$ (sec^{-1})	0°			90°		
	r (%)	T_R (sec)	T_1' (sec)	r (%)	T_R (sec)	T_1' (sec)
0.001	9.2	15.4	18.9	7.2	18.0	20.2
0.005	36.6	12.0	21.5	31.5	14.5	21.7
0.01	57.6	9.5	24.4	52.6	11.3	23.8
0.02	78.7	6.7	29.4	75.5	7.8	27.9
0.03	87.9	5.1	33.2	85.9	5.9	31.3
0.04	92.5	4.1	36.1	91.2	4.7	33.9
0.1	98.6	1.8		98.4	2.0	
1.0	100	<0.3		100	<0.3	

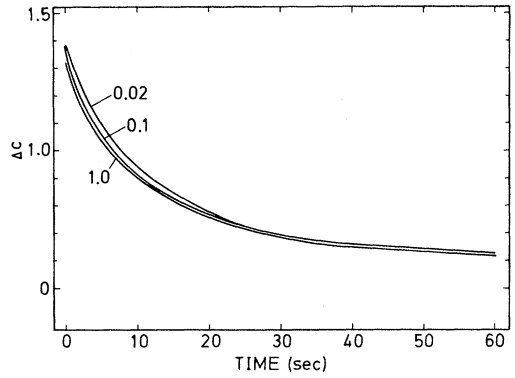

FIG. 4. Time dependence of Δc for $1/T=100\ \mathrm{K}^{-1}$. The respective strength of the rf power, $B^{\mathrm{rf}}/\Delta f_t$, is given beside each curve (unit: sec^{-1}). For large rf power ($B^{\mathrm{rf}}/\Delta f_t=1\ \mathrm{sec}^{-1}$), $\Delta c(t\to 0)$ and $\Delta c(t\to\infty)$ coincide well with Δc^{SRL} and Δc^{FRL}.

tions, the sweep-up-down results for $\overline{c(0)}$ and $\overline{\Delta c}$ cannot be calculated averaging the results for sweep-up and sweep-down.) Here sweep-up means that the energetically lowest sublevel transition is entered first. Figure 7 shows $\overline{c(0)}$ and $\overline{\Delta c}$ for $1/T=100\ \mathrm{K}^{-1}$ versus Δt. The variation of $\overline{c(0)}$ is relatively strong, while the dependence of $\overline{\Delta c}$ on Δt is relatively weak, especially for sweep-mode technique.

Figure 8 illustrates the behavior of $\overline{c(0)}$ and $\overline{\Delta c}$

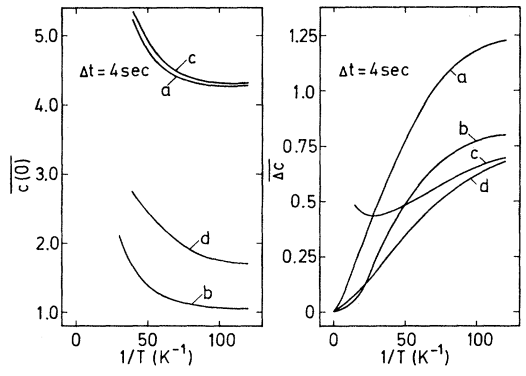

FIG. 5. $\overline{c(0)}$ and $\overline{\Delta c}$ versus $1/T$ for a measurement time $\Delta t=4$ sec. ($B^{\mathrm{rf}}/\Delta f_t=0.1\ \mathrm{sec}^{-1}$.) The labels *a,b,c,d* have the following meaning: *a*: no-sweep technique, i.e., the system is allowed to relax to the thermal equilibrium between measurements at different frequencies. *b*: sweep technique, sweep-up. Here sweep-up means that the energetically lowest sublevel transition is entered first. *c*: sweep technique, sweep-down. *d*: sweep technique, sweep-up-down.

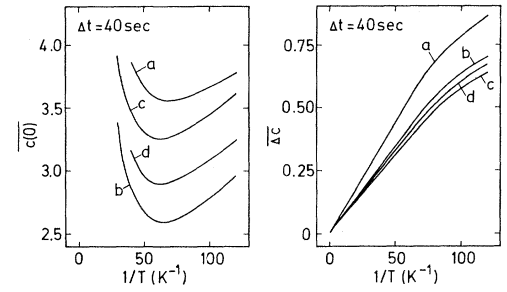

FIG. 6. $\overline{c(0)}$ and $\overline{\Delta c}$ versus $1/T$ for a measurement time $\Delta t=40$ sec. ($B^{\mathrm{rf}}/\Delta f_t=0.1\ \mathrm{sec}^{-1}$). For the explanation of *a,b,c,d*, see Fig. 5. The differences between sweep-up (curve *b*) and sweep-down (curve *c*) become smaller for longer measurement times.

on the rf power. The weak dependence, which is a rather surprising result, indicates that a precise knowledge of $B^{\mathrm{rf}}/\Delta f_t$ is not necessary for the interpretation of measured resonance displacements.

V. SUMMARY AND OUTLOOK

It has been shown that magnitude *and* sign of a small quadrupole splitting superimposed to the hyperfine splitting in a ferromagnetic material can be determined from the $0°-90°$ differential resonance displacement. This is a "stand-alone" technique; i.e., all parameters necessary for the interpretation of DRD data can be measured with the same experimental setup. The A_2, A_4 coefficients are obtained from the absolute values of the γ anisotropies measured at $\theta=0°$ and $90°$. The rf and the relaxation parameters B^{rf} and B^{SL}, respectively, can be determined by observing the time dependence of

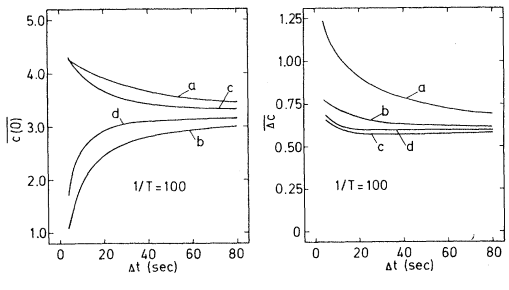

FIG. 7. $\overline{c(0)}$ and $\overline{\Delta c}$ versus measurement time. ($B^{\mathrm{rf}}/\Delta f_t=0.1\ \mathrm{sec}^{-1}$; $1/T=100\ \mathrm{K}^{-1}$). For sweep-mode technique the dependence of $\overline{\Delta c}$ on Δt is small. (See Fig. 5 for explanation of *a,b,c,d.*)

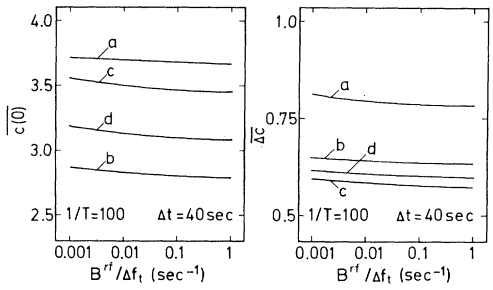

FIG. 8. $\overline{c(0)}$ and $\overline{\Delta c}$ versus $B^{rf}/\Delta f_t$ ($\Delta t=40$ sec; $1/T=100$ K^{-1}). The weak dependence of $\overline{c(0)}$ and $\overline{\Delta c}$ on $B^{rf}/\Delta f_t$ is a surprising result; this has the consequence that no free parameter is necessary for the analysis of data on the $0°-90°$ resonance displacement. (See Fig. 5 for explanation of *a,b,c,d*.)

the γ anisotropy after a resonant rf field is switched on and off. As the DRD is nearly independent on the rf power, no care has to be taken to determine the effective rf power at the impurity sites, which would be difficult as B^{rf} is expected to vary considerably within the sample because of the finite skin depth. This means that *no* free parameter is necessary for the intepretation of DRD data. The DRD is most efficiently measured utilizing the sweep-mode technique. By the choice of different sweep rates and modulation widths, reliable cross checks can be performed. The sweep technique also allows the determination of ν_Q if the DRD vanishes, the latter being the case for all γ transitions with $A_4=0$.

Using hcp Co as host lattice it should be possible to measure the quadrupole splitting of a large series of radioactive nuclei. For isotopic chains it is then possible to derive ratios of quadrupole moments. In comparison to adiabatic fast passage[14] it is a decisive advantage that no free parameter has to be fitted in the analysis of data.

ACKNOWLEDGMENTS

I am indebted to Professor P. Kienle for his continuous interest and support of this work. I also wish to thank Dr. E. Zech for discussions. This work was supported by the Bundesministerium für Forschung und Technologie, Bonn.

[1]G. N. Rao, Hyperfine Interact. 7, 141 (1979).
[2]E. Matthias and R. J. Holliday, Phys. Rev. Lett. 17, 897 (1966).
[3]P. Herzog, Hyperfine Interact. 8, 215 (1980).
[4]E. Hagn, K. Leuthold, E. Zech, and H. Ernst, Z. Phys. A 295, 385 (1980).
[5]E. Hagn and E. Zech, following paper, Phys. Rev. B 25, 1529 (1982).
[6]S. R. de Groot, H. A. Tolhoek, and W. J. Huiskamp, in *Alpha-, Beta-, and Gamma-Ray Spectroscopy,* edited by K. Siegbahn (North-Holland, Amsterdam, 1965), Vol. 2, p. 1199,
[7]T. Yamazaki, Nucl. Data. Sect. A 3, 1 (1967).
[8]P. D. Johnston, R. A. Fox, and N. J. Stone, J. Phys. C 5, 2077 (1972).
[9]F. Bacon, J. A. Barclay, W. D. Brewer, D. A. Shirley, and J. E. Templeton, Phys. Rev. B 5, 2397 (1972).
[10]K. Leuthold, E. Hagn, H. Ernst, and E. Zech, Phys. Rev. C 21, 2581 (1980).
[11]H. Enokiya, J. Phys. Soc. Jpn. 42, 796 (1977).
[12]M. Kawakami, T. Hihara, Y. Koi, and T. Wakiyama, J. Phys. Soc. Jpn. 33, 1591 (1972).
[13]A. Abragam, *The Principles of Nuclear Magnetism* (University Press, Oxford, 1961), p. 363.
[14]P. T. Callaghan, P. D. Johnston, and N. J. Stone, J. Phys. C 7, 3161 (1974).